ARTICLE

Check for updates

Journal of
Sensor Science and Technology

The Korean Sensors Society

High-Sensitivity NO_2 Gas Sensor Based on PbS Quantum Dots with WO_3 Nanoparticle Catalytic Layer

Jinbeom Kwon[1,+]

[1]*Department of Semiconductor Engineering, Kyungwoon University, 730, Gangdong-ro, Sandong-eup, Gumi-si, Gyeongsangbuk-do 39160, Republic of Korea*

Cite This: *J. Sens. Sci. Technol. Vol. 34, No. 6 (2025) 645-650*

https://doi.org/10.46670/JSST.2025.34.6.645

ABSTRACT: With the rapid pace of industrial development intensifying air pollution and greenhouse gas emissions, the resulting acceleration of global warming has increased the need for advanced technologies to mitigate these effects. Among various greenhouse gases, nitrogen dioxide (NO_2), primarily emitted from automobile exhaust and industrial processes, is recognized as a significant contributor to global warming. Although semiconductor-type NO_2 gas sensors based on metal oxides, such as SnO_2 and ZnO, have been extensively investigated, they face challenges, including high fabrication costs, high power consumption due to elevated operating temperatures, and poor gas selectivity, which hinder accurate NO_2 detection. Meanwhile, PbS quantum dots (QDs)-based gas sensors have recently attracted attention for their high selectivity toward NO_2 even at low operating temperatures. However, compared to conventional metal oxide-based sensors, their sensitivity, detection limit, and response speed still require significant improvement. To overcome these limitations, this study introduces WO_3 nanoparticles as catalysts to enhance the sensitivity and response speed of PbS QDs-based NO_2 sensors. The optimized sensor, fabricated via screen printing, accurately detected NO_2 gas concentrations ranging from 1 ppm to 200 ppb, with a resolution of 200 ppb at room temperature. Furthermore, the developed sensor exhibited approximately 3.25 times higher sensitivity and 18.7% faster response speed compared with the sensor without WO_3 catalysts.

KEYWORDS: *Quantum dots, PbS, NO_2, Gas sensor*

1. INTRODUCTION

With rapid industrialization, greenhouse gas emissions have significantly increased, thereby accelerating air pollution and global warming. Nitrogen dioxide (NO_2) is a significant air pollutant primarily generated by vehicle exhaust, fossil fuel combustion, and industrial processes [1-3]. NO_2 contributes to global warming and poses serious health hazards, including respiratory and cardiovascular diseases [4]. Prolonged exposure can lead to bronchial inflammation, asthma, or impaired lung function, while even low concentrations can cause long-term health effects. Due to these risks, the World Health Organization (WHO) has imposed strict limits on atmospheric NO_2 concentrations, highlighting the need for accurate and reliable detection technologies [5]. Semiconductor-type NO_2 gas sensors based on metal oxides, such as SnO_2 and ZnO, have been widely investigated owing to their high sensitivity and simple structure [6,7]. However, their high operating temperature requirements result in high power consumption, complex fabrication processes, and poor gas selectivity, limiting their use in low-power, room-temperature applications such as indoor monitoring and wearable devices [8-10].

Recently, PbS quantum dots (QDs)-based materials have emerged as promising candidates for next-generation gas sensors [11-13]. PbS QDs possess a tunable bandgap and highly modifiable surface chemistry, allowing the control of charge transport and surface reactions [14]. Consequently, they have high reactivity and selectivity toward NO_2 at low temperatures [15]. Nevertheless, conventional PbS QDs sensors still have limitations in terms of sensitivity, response speed, and long-term stability, necessitating further improvement. This study formed a catalytic layer using WO_3 nanoparticles (NPs) to enhance the sensing performance of PbS QDs-based NO_2 gas sensors [16-19]. WO_3 acts as an n-type semiconductor catalyst and electron donor that facilitates

[+]Corresponding author: jinbum0301@ikw.ac.kr
Received : Oct. 16, 2025, Revised : Oct. 27, 2025, Accepted : Oct. 31, 2025

charge transfer and accelerates redox reactions with NO_2 molecules. In addition, the p–n heterojunction formed between WO_3 (n-type) and PbS QDs (p-type) promotes efficient charge separation and suppresses electron–hole recombination, resulting in enhanced sensitivity and response speed [17,18]. The incorporation of WO_3 optimizes the charge transport pathways within the WO_3–PbS composite, improving signal stability and enabling reliable room-temperature operation [19]. The optimized sensor, fabricated by screen printing, precisely detected NO_2 concentrations from 1 ppm to 200 ppb with a resolution of 200 ppb, exhibiting 3.25 times higher sensitivity and 18.7% faster response than the sensor without WO_3 [20]. Overall, this study presents a low-power, room-temperature-operable NO_2 gas sensor based on the PbS QDs/WO_3 bilayer structure, offering a promising approach for environmental monitoring, industrial safety, and wearable electronic applications.

2. EXPERIMENTAL

2.1 Synthesis of PbS Quantum Dots

PbS QDs were synthesized using a refined colloidal synthesis route [11]. To prepare the sulfur precursor, 0.032 g of elemental sulfur was dispersed in 2.4 mL of oleylamine (OLA) and stirred under a nitrogen atmosphere for 30 min at room temperature until a uniform solution was obtained. The lead precursor was prepared by dissolving 0.417 g of lead(II) chloride ($PbCl_2$) in 5 mL of OLA, followed by stirring under nitrogen for 30 min at room temperature. The solution was then heated to 160°C and maintained at this temperature for 1 h to ensure complete dissolution and precursor complexation. To remove residual volatiles and impurities, the lead precursor was subsequently degassed under vacuum at 120°C for 15 min. After degassing, the reaction temperature was adjusted to 110°C. Then, 275 µL of the sulfur–OLA solution and 274 µL of trioctylphosphine were quickly injected into the $PbCl_2$–OLA mixture under nitrogen flow, inducing immediate nucleation and growth of PbS QDs. The reaction mixture was maintained at this temperature for 30 min, and then cooled to room temperature naturally. For purification, the crude product was washed with methanol and toluene in a 4:1:1 volume ratio, followed by centrifugation at 3000 rpm for 5 min to separate the QDs from the unreacted precursors and byproducts. The collected nanoparticles were redispersed in toluene to yield a stable colloidal PbS QD solution with a final concentration of approximately 20 mg/mL^{-1}.

2.2 Synthesis of PbS QDs & WO_3 NPs paste

For screen printing, both PbS QDs and WO_3 NPs pastes were prepared [1,4]. The PbS QDs paste was formulated by mixing 1 mL of the synthesized PbS QDs colloidal solution (20 mg/mL^{-1}) with 30 mg of ethyl cellulose (EC) as a binder. The mixture was magnetically stirred at room temperature for 3 h until a homogeneous viscous paste suitable for uniform film deposition was obtained. Similarly, a WO_3 NPs paste was prepared by dispersing 30 mg of WO_3 NPs in 1 mL of ethanol, followed by the addition of 30 mg of ethyl cellulose. The WO_3 NPs suspension was stirred thoroughly at room temperature for 4 h until complete dissolution of the binder and uniform particle dispersion were achieved [5,6].

2.3 Fabrication of PbS QDs–based NO_2 gas sensor

The NO_2 gas sensor was fabricated via screen printing [19]. The alumina substrates (5 × 5 mm^2) were cleaned sequentially with acetone, methanol, and isopropyl alcohol to remove surface contaminants. The interdigitated (IDE) silver electrodes were then patterned on the cleaned substrates by screen printing with commercial silver paste and were subsequently dried. To form the catalytic layer, a WO_3 NPs paste was deposited onto the IDE region using a 1.5 × 1.5 mm^2 shadow mask, following the same screen-printing process. The printed WO_3 layer was annealed at 150°C for 1 h in air to ensure uniform adhesion and to remove any residual organic compounds. After cooling to room temperature, the PbS QDs paste was printed directly on top of the WO_3 layer through a 3 × 3 mm^2 shadow mask, defining the active sensing area of the device. The printed films were then annealed at 90°C for 30 min to eliminate solvent residues and enhance interparticle connectivity. For comparison, a reference device was fabricated under identical processing conditions without a WO_3 catalytic layer, in which only the PbS QDs paste was printed onto the silver IDE using the same 3 × 3 mm^2 shadow mask. The fabricated devices, comprising the WO_3/PbS QDs composite gas sensor and the PbS QDs-only reference device, featured an overall active sensing region of 9 mm^2, enabling

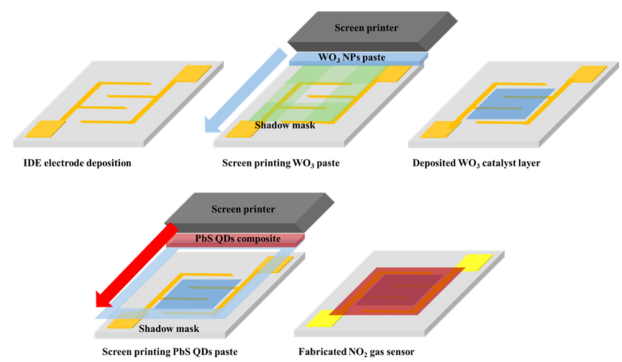

Fig. 1. Schematic diagram of the fabrication of an NO_2 gas sensor based on PbS QDs

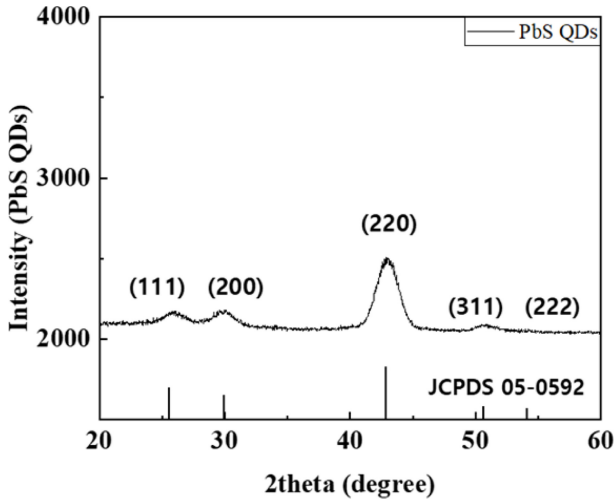

Fig. 2. XRD analysis characteristics of synthesized PbS QDs.

direct evaluation of the catalytic enhancement effect of the WO_3 interlayer on the NO_2 gas sensor performance.

3. RESULTS AND DISCUSSIONS

3.1 Characteristics of the synthesized PbS QDs

The crystalline structure and particle size of the synthesized PbS QDs were analyzed using X-ray diffraction (XRD). For sample preparation, a 20 $mgmL^{-1}$ PbS QD solution was spin coated onto 10×10 mm^2 alumina substrates at 1000 rpm for 30 s, followed by thermal annealing at 95°C for 30 min to remove residual solvent and improve film uniformity. As shown in Fig. 2, the XRD pattern exhibited distinct diffraction peaks at 25.8°, 30.1°, and 43.1°, which correspond to the (111), (200), and (220) planes of cubic PbS, respectively. These peak positions agree well with the reported values for rock-salt-type PbS, confirming that the synthesized QDs possess high crystallinity and phase purity [9,10]. This well-defined crystal structure indicates that PbS QDs can provide a stable, uniform sensing layer, essential for reliable gas-sensing performance. The crystallite sizes of the PbS QDs were estimated from the XRD results using the Scherrer equation:

$$D_{hkl}(\text{nm}) = (\text{K} * \lambda)/\beta\cos\theta, \quad (1)$$

where K is the Scherrer constant, λ is the wavelength of the incident X-ray, β is the full width at half maximum (FWHM) of the selected diffraction peak (in radians), and θ is the Bragg angle. The parameters used for the calculation were K = 0.94 (for spherical crystallites with cubic symmetry), θ = 15.1°, FWHM = 1.74°, and λ = 0.15418 nm (Cu Kα radiation). Based on these values, the average crystallite size of the PbS QDs is approximately 5.2 nm [1]. The nanoscale grains provided a large effective surface area, which facilitated gas adsorption and enhanced the chemical reactivity of the film [3,14]. Therefore, the fine crystallinity and reduced particle size of the PbS QDs are expected to significantly enhance NO_2 sensing sensitivity and accelerate response kinetics in the fabricated gas sensor devices.

3.2 Characteristics of the fabricated NO_2 gas sensor

The gas-sensing performance of the fabricated PbS QDs NO_2 sensors was evaluated in a closed gas chamber under controlled conditions. NO_2 gas (1 ppm, air-balanced) was diluted with pure air using a mass flow controller to precisely adjust the concentration. The total gas flow rate was maintained at 1000 sccm, and all measurements were conducted at a constant operating temperature of 80°C, controlled by a ceramic heater. A source-measurement unit was used to monitor the real-time current–voltage characteristics of the devices. Each measurement cycle consisted of 1 min of NO_2 injection and 2 min of air purging for the response and recovery processes, respectively.

The NO_2 concentration was decreased stepwise from 1 ppm to 200 ppb with a measurement resolution of 200 ppb, enabling precise evaluation of the sensor's current modulation behavior as a function of gas concentration. Fig. 3(a) and (b) show the real-time current variation of the sensors as the NO_2 concentration decreased from 1 ppm to 200 ppb. As the gas concentration decreased, the current gradually decreased, exhibiting a clear concentration-dependent trend. The maximum current modulation was observed at 1 ppm NO_2. At this concentration, the PbS QDs single device (reference) exhibited a current change (ΔI) of 2.08 μA, whereas the WO_3 nanoparticles (NPs)–modified device showed a significantly larger current change of 4.21 μA, indicating approximately a 2.02-fold higher current modulation compared with the pristine PbS QDs sensor [16,17]. The current variation was quantitatively expressed as response (%), which was calculated using Eq. (2).

$$\text{Response } (\%) = \frac{I_{res} - I_{rec}}{I_{rec}} \times 100 \quad (2)$$

Here, I_{res} and I_{rec} represent the current during gas exposure (response) and air purging (recovery), respectively. As shown in Fig. 3(c), the WO_3 NP-coated device exhibited a 3.25-fold higher response than the unmodified PbS QDs sensor [18,19]. This definition reflects the relative current variation induced by NO_2 adsorption and desorption. The enhanced current response of the WO_3/PbS QDs composite

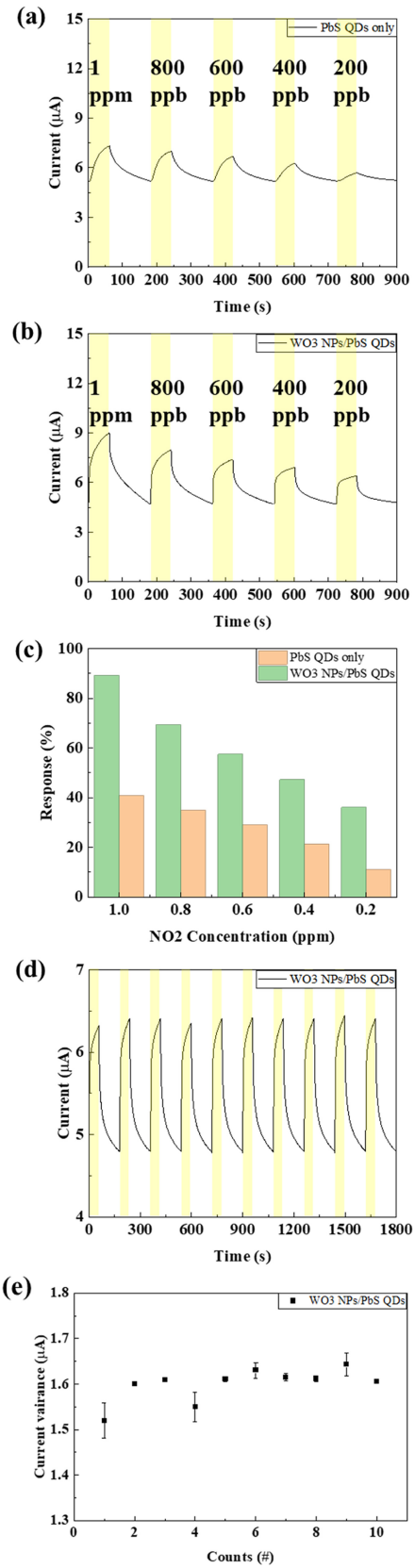

Fig. 3. Real-time current variation of (a) PbS QDs reference sensor and (b) WO_3/PbS QDs–based sensor at various NO_2 concentrations; (c) Comparison of sensor responses; (d) Repeated measurements, and (e) Error rate of the WO_3/PbS QDs sensor.

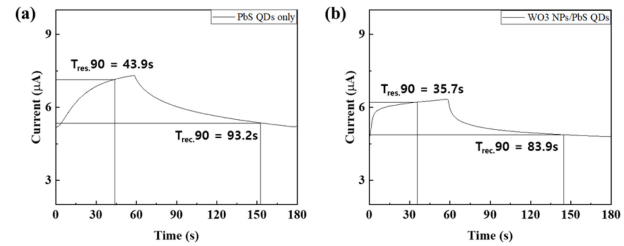

Fig. 4. Response and recovery time measurement curves of the fabricated NO_2 gas sensors: (a) PbS QDs sensor and (b) WO_3NPs/PbS QDs composite sensor.

Table 1. Performance comparison of PbS QDs and WO_3/PbS QDs-based gas sensors

Parameter	PbS QDs	WO_3/PbS QDs
Current change @ 1 ppm	2.08 μA	4.21 μA
Maximum response (%)	-	3.25 × higher
Response time (s)	43.9 s	35.7 s
Recovery time (s)	93.2 s	83.9 s
Deviation @ 1 ppm	—	< 4%

sensor can be attributed to the catalytic and electronic effects of the WO_3 layer, which promoted charge transfer and accelerated the oxidation–reduction reaction of NO_2, leading to amplified current modulation during gas exposure. The response time and recovery time were determined as the times required for the current to reach 90% of its steady-state value after gas exposure and air purging, respectively. As shown in Fig. 4, the PbS QDs reference device exhibited a minimum response time of 43.9 s and a recovery time of 93.2 s, whereas the WO_3/PbS QDs composite device showed faster dynamics, with a response time of 35.7 s and a recovery time of 83.9 s. Accordingly, the composite device demonstrated an 18.7% faster response and a 10.0% improvement in recovery speed compared with the reference. These improvements are attributed to the WO_3 layer, which facilitates electron transport and accelerates NO_2 adsorption–desorption kinetics on the PbS surface. As a result, the WO_3/PbS QDs heterostructure enhanced the charge transfer efficiency, leading to improved response performance and signal stability [16-18]. To verify the reliability and repeatability of the sensors, they were tested for ten consecutive cycles under 200 ppb NO_2 exposure. As shown in Fig. 3(d) and (e), the WO_3/PbS QDs composite sensor exhibited highly consistent response and recovery behavior with less than 4% deviation, confirming its excellent reproducibility and long-term stability. The superior sensing performance of the WO_3/PbS QDs device originated from the synergistic effects between the catalytic activity and electronic modulation of the WO_3 layer. WO_3, acting as an n-

type catalytic semiconductor, forms a p–n heterojunction with p-type PbS QDs, which enhances charge separation and suppresses electron–hole recombination [17-19]. Furthermore, the catalytic surface of WO_3 accelerates the redox interactions with NO_2 molecules, thereby amplifying the conductivity change in the PbS layer. Consequently, the WO_3/PbS QDs composite sensor achieved enhanced sensitivity, faster response and recovery, and superior signal stability compared with the pristine PbS QDs sensor.

4. CONCLUSIONS

This study successfully synthesized PbS QDs with a rock-salt cubic structure and an average crystallite size of approximately 5.2 nm, as confirmed by XRD analysis. The nanoscale grain size and high crystallinity of QDs provide a large active surface area and a stable structural framework suitable for gas-sensing applications. To enhance sensing performance, a WO_3 catalytic layer was incorporated beneath the PbS QDs to form a WO_3/PbS QDs heterostructure. The fabricated NO_2 sensors were systematically evaluated at concentrations ranging from 1 ppm – 200 ppb with a measurement resolution of 200 ppb. The composite device exhibited a significantly larger current change (4.21 μA) than the pristine PbS QDs sensor (2.08 μA) at 1 ppm NO_2, corresponding to a 3.25-fold higher response. Moreover, the WO_3/PbS QDs sensor achieved faster response and recovery times of 35.7 s and 83.9 s, respectively—representing improvements of 18.7% and 10.0% compared with the reference. The sensor also demonstrated excellent repeatability, with less than 4% deviation over ten consecutive cycles. These results indicate that the synergistic catalytic and electronic effects of WO_3 effectively enhanced charge transport and accelerated the adsorption–desorption kinetics of NO_2, leading to higher sensitivity and improved stability. Thus, the WO_3/PbS QDs heterostructure provides a promising platform for developing low-power, high-performance gas sensors that are operable at near-room temperatures. This approach may be further extended to other nanocomposite systems for environmental monitoring, industrial safety, and smart-device applications.

CRediT Authorship Contribution Statement

Jinbeom Kwon conducted all aspects of the research and manuscript preparation.

Declaration of Competing Interest

The authors declare that they have no competing financial interests or personal relationships that may have influenced the work reported in this study.

Acknowledgements

This research received no external funding.

REFERENCES

[1] J. Kwon, Y. Ha, S. Choi, D.G. Jung, H.k. An, S.H. Kong, et al., Solution-processed NO_2 gas sensor based on poly(3-hexylthiophene)-doped PbS QDs operable at room temperature, Sci. Rep. 14 (2024) 20600.

[2] Z. Hu, L. Zhou, L. Li, J. Liu, H.-Y. Li, B. Song, et al., Stabilization of PbS colloidal-quantum-dot gas sensors using atomic-ligand engineering, Sens. Actuators B Chem. 388 (2023) 133850.

[3] A. Mirzaei, Z. Kordrostami, M. Shahbaz, J.-Y. Kim, H.W. Kim, S.S. Kim, Resistive-based gas sensors using quantum dots, Sensors 22 (2022) 4369.

[4] F. Mitri, A. De Iacovo, M. De Luca, A. Pecora, L. Colace, Lead sulphide colloidal quantum dots for room-temperature NO_2 gas sensors, Sci. Rep. 10 (2020) 12556.

[5] X. Xin, Y. Zhang, X. Guan, J. Cao, W. Li, X. Long, et al., Enhanced performances of PbS quantum-dots-modified MoS_2 composite for NO_2 detection at room temperature, ACS Appl. Mater. Interfaces 11 (2019) 9438.

[6] X. Li, L. Fu, H. Karimi-Maleh, F. Chen, S. Zhao, Innovations in WO_3 gas sensors: nanostructure engineering, functionalization, and future perspectives, Heliyon 10 (2024) e27740.

[7] Y. Wang, J. Li, D. Xiao, D. Zhang, Y. Liu, M. Sun, et al., Progress in functionalized WO_3-based gas sensors for selective H_2S and NH_3: a review, Ceram. Int. 50 (2024) 40631.

[8] G. Feng, S. Wang, S. Wang, P. Wang, C. Wang, Y. Song, et al., Ultra-sensitive trace NO_2 detection based on quantum dots-sensitized few-layer MXene: a novel convincing insight into dynamic gas-sensing mechanism, Sens. Actuators B Chem. 400 (2024) 134852.

[9] S.S. Nalimova, Z.V. Shomakhov, O.D. Zyryanova, V.M. Kondratev, C.D. Bui, S.A. Gurin, et al., WO_{3-x}/WS_2 nanocomposites for fast-response room-temperature gas sensing, Molecules 30 (2025) 566.

[10] Y. Masuda, A. Uozumi, Highly responsive diabetes and asthma sensors with WO_3 nanoneedle films for the detection of biogases with low concentrations, NPG Asia Mater. 15 (2023) 69.

[11] Z. Wei, L. Xu, S. Peng, Q. Zhou, Application of WO_3 hierarchical structures for the detection of dissolved gases in transformer oil: a mini review, Front. Chem. 8 (2020) 188.

[12] M. Modak, S. Rane, S. Jagtap, WO_3: a review of synthesis techniques, nanocomposite materials and their morphological effects for gas sensing application, Bull. Mater. Sci. 46 (2023) 28.

[13] S.R. Sriram, S. Parne, V.S.C.S. Vaddadi, D. Edla, N.P., R.R. Avala, et al., Nanostructured WO_3-based gas sensors: A short review, Sensor Rev. 41 (2021) 406–424.

[14] S. Hambir, S. Jagtap, Nitrogen dioxide gas-sensing properties of hydrothermally synthesized $WO_3 \cdot nH_2O$ nanostructures, R. Soc. Open Sci. 10 (2023) 221135.

[15] K. Ganesan, P.K. Ajikumar, Unusual gas sensor response and semiconductor-to-insulator transition in WO_{3-x} nanostructures: The role of oxygen vacancies, Surf. Interfaces 65 (2025) 106433.
[16] Y.C. Chiu, M. Deb, P.T. Liu, H.W. Zan, Y.R. Shih, Y. Kuo, et al., Sputtered Ultrathin WO_3 for Realizing Room-Temperature High-Sensitive NO_2 Gas Sensors, ACS Appl. Electron. Mater. 5 (2023) 5831–5840.
[17] W. Fanga, Y. Yang, H. Yua, X. Dong, T. Wanga, J. Wang, et al., One-step synthesis of flower-shaped WO_3 nanostructures for a high-sensitivity room-temperature NO_x gas sensor, RSC Adv. 6 (2016) 106880–106886.
[18] J. Han, W. Zhou, D. Kong, Y. Gao, Y. Gao, Y. Wang, G. Lu, High-performance NO_2 gas sensor enabled by Fe, N co-doped GQDs modification and pulse-driven temperature modulation, Sens. Actuators B Chem. 417 (2024) 136040.
[19] M. Ganesan, S. Harish, K. Shanmugasundaram, M.K. Mohan, J. Archana, M. Navaneethan, Highly sensitive and selective Au-loaded WO_3 nanoplates for NO_2 gas detection, Sens. Actuators B Chem. 440 (2025) 137900.
[20] J. Bai, Y. Shen, A. Li, M. Wu, H. Xiao, Q. Zhao, S. Zhao, W. Liu, B. Cui, Design of PbS quantum dots–$PbMoO_4$–MoS_2 ternary nanocomposites for highly selective NO_2 sensing at room temperature, Int. J. Miner. Metall. Mater. 32 (2025) 1771–1782.